Cell, Vol. 94, 427–438, August 21, 1998, Copyright ©1998 by Cell Press

Structure of the Histone Acetyltransferase Hat1: A Paradigm for the GCN5-Related N-acetyltransferase Superfamily

Robert N. Dutnall,* Stefan T. Tafrov,† Rolf Sternglanz,† and V. Ramakrishnan*‡
*Department of Biochemistry
University of Utah School of Medicine
Salt Lake City, Utah 84132
†Department of Biochemistry and Cell Biology
SUNY
Stony Brook, New York 11794

Summary

We have solved the crystal structure of the yeast histone acetyltransferase Hat1–acetyl coenzyme A (AcCoA) complex at 2.3 Å resolution. Hat1 has an elongated, curved structure, and the AcCoA molecule is bound in a cleft on the concave surface of the protein, marking the active site of the enzyme. A channel of variable width and depth that runs across the protein is probably the binding site for the histone substrate. A model for histone H4 binding by Hat1 is discussed in terms of possible sources of specific lysine recognition by the enzyme. The structure of Hat1 provides a model for the structures of the catalytic domains of a protein superfamily that includes other histone acetyltransferases such as Gcn5 and CBP.

Introduction

The reversible acetylation of specific lysine residues within the N-terminal tails of the core histones is of considerable interest since it has been known for some time that levels of histone acetylation are correlated with gene activity (reviewed in Turner, 1998). For example, potentially active euchromatin is associated with hyperacetylated histones, whereas inactive heterochromatin is associated with hypoacetylated histones. Recently there has been a resurgence of interest in histone acetylation following the identification of genes for several histone acetylase (HAT) and histone deacetylase (HDAC) enzymes. Many of these genes turned out to be previously identified transcriptional coactivator or repressor proteins providing a link between histone acetylation and transcription (reviewed in Grunstein, 1997; Kadonaga, 1998; Struhl, 1998).

Histone acetylation, particularly of histone H4, has also been proposed to play an important role in replication-dependent nucleosome assembly (reviewed in Brownell and Allis, 1996; Kaufman, 1996; Roth and Allis, 1996). Newly synthesized histone H4 is acetylated specifically at Lys-5 and Lys-12 in many species ranging from *Tetrahymena thermophila* to humans (Sobel et al., 1995). Newly synthesized histone H3 is also acetylated but the pattern is less conserved (Sobel et al., 1995; Kuo et al., 1996). Following the import of new histones H3 and H4 into the nucleus, and assembly onto DNA, their acetylation pattern is altered by the action of nuclear histone acetylases and deacetylases. It has been found that chromatin assembly factor 1 (CAF-1), which assembles H3/H4 tetramers onto replicating DNA in vitro, forms a stable complex with newly synthesized H3/H4 tetramers that display a specific pattern of acetylation (Verreault et al., 1996). The association of CAF-1 with specifically modified histones suggests that acetylation may be important for targeting histones to replicating DNA or for nucleosome assembly (Verreault et al., 1996).

The *Saccharomyces cerevisiae HAT1* gene was the first HAT gene to be identified and has been shown to acetylate specifically residue Lys-12 of histone H4 (Kleff et al., 1995; Parthun et al., 1996). Hat1 purified from yeast cytoplasmic extracts was found to be tightly associated with an accessory protein, Hat2, which enhances the activity of Hat1 by increasing its affinity for histone H4 (Parthun et al., 1996). Recently a human homolog of Hat1 has been described that is capable of acetylating histone H4 at Lys-5 and Lys-12 and also Lys-5 of histone H2A to a lesser extent (Verreault et al., 1998). Like its yeast counterpart, human Hat1 is associated with an accessory protein, RbAp46, which also stimulates the activity of the catalytic subunit (Verreault et al., 1998). Hat2 and RbAp46 are members of the WD-repeat family of proteins (Neer et al., 1994), which also includes the p48 subunit of CAF-1 (Kaufman et al., 1997). RbAp46 and CAF-1 p48 have both been shown to interact with histone H4 (Verreault et al., 1996, 1998). A HAT enzyme has been identified in maize embryo cytoplasmic extracts, HatB, which specifically acetylates histone H4 at Lys-5 and Lys-12 and which shares significant sequence similarity with Hat1 (Eberharter et al., 1996; Kolle et al., 1998). This enzyme is also apparently part of a complex with a partner protein of similar size to Hat2 and RbAp46 (Eberharter et al., 1996).

Hat1 was originally described as a B-type HAT (Brownell and Allis, 1996), based on its purification from cytoplasmic extracts and the observation that it is incapable of modifying H4 incorporated in nucleosomes (Parthun et al., 1996). However, immunological staining indicates that both human and yeast Hat1 are primarily localized in the nucleus (Verreault et al., 1998; S. T. T. and R. S., unpublished data). Intriguingly, it has been reported that Hat1 forms part of two HAT complexes in yeast, one of which is localized in the nucleus and the other in the cytoplasm (Ruiz-García et al., 1998). A possible Hat1 homolog has also been described in *Tetrahymena*, which can acetylate histone H4 Lys-4 and Lys-11 (equivalent to yeast Lys-5 and Lys-12) and which is apparently present in both the cytoplasm and micronuclei (Richman et al., 1988).

Based on the modifications of histone H4 produced by the yeast, human, and maize enzymes, Hat1 is likely to be involved in generating the modified H4 required for replication-dependent chromatin assembly. Further support for this role is the observation that the activity of the maize HatB enzyme is closely linked to DNA synthesis during germination of maize embryos (Eberharter

‡To whom correspondence should be addressed.

et al., 1996). It has been proposed that the yeast nuclear Hat1 complex could be involved in regenerating the acetylation pattern required to assemble nucleosomes independently of replication (for example, to reassemble nucleosomes in regulatory regions or following repair processes) (Ruiz-García et al., 1998). Hat1 could also be involved in generating or maintaining the histone H4 Lys-12 acetylation typical of yeast heterochromatin (Grunstein, 1997). However, deletion of the *HAT1* or *HAT2* genes produces no apparent phenotype (Kleff et al., 1995; Parthun et al., 1996; Ruiz-García et al., 1998), although this is usually credited to the presence of other HAT enzymes that modify histone H4.

We describe the crystal structure of the HAT domain of yeast Hat1 complexed with its cofactor acetyl coenzyme A. Hat1 is a member of a superfamily of acetyltransferase enzymes of diverse function that includes several other HAT enzymes (Neuwald and Landsman, 1997). We discuss the implications of the structure for activity and substrate recognition, and its relationship to the structures of other HAT enzymes including Gcn5 and CBP.

Results and Discussion

Identification of a Minimal HAT Domain of Hat1 and Structure Determination

Full-length recombinant Hat1 expressed in bacteria yielded crystals that grew over several months and diffracted at best to 7 Å resolution. We therefore used a combination of limited proteolysis and HAT activity assays to identify a smaller catalytically active fragment of Hat1 (Dutnall et al., submitted). These studies revealed that the C-terminal 54 residues of Hat1 can be deleted without reducing HAT activity in vitro. Based on this result, we expressed and purified a Hat1 construct containing only residues 1–320, which yielded crystals in the presence of AcCoA that diffract to $\sim$2 Å resolution.

We solved the structure of the complex of Hat1(1–320) with AcCoA using multiwavelength anomalous diffraction on a single crystal of selenomethionine-substituted protein (this protein will be referred to as Hat1). Statistics for the structure determination and refinement are summarized in Table 1. The current model contains 306 of the 319 residues of the protein (N-terminal sequencing and mass spectrometry showed that the N-terminal methionine is absent). Residues 2–5 and 200–208 have not been included in the model as no electron density could be located for these regions. The poorest parts of the model are a loop at residues 284–289 and the C-terminal residues 319–320. Only weak main-chain density could be observed for these residues, and they were modeled as alanines. For the AcCoA, electron density is poorly defined for the ribose sugar and adenine base, and these have been only tentatively placed in the model.

Overview of the Protein Structure

Hat1 is composed of a mixture of helices and sheets with overall dimensions of around 70 Å $\times$ 60 Å $\times$ 20–40 Å. As shown in Figure 1, it can be seen that the structure is elongated, adopting a curved shape such that the N and C termini lie at opposite ends of the structure. Hat1 can be divided into two domains that are connected by an extended loop: an N-terminal domain from residues 2 to 111 and a C-terminal domain from residues 122 to 320 (which contains the AcCoA binding site). A hydrophobic interface is formed between the two domains. A structural homology search performed with the whole protein as well as with the separate N- and C-terminal domains showed no significant overall similarity with other known proteins present in current databases including several structures of CoA binding proteins (Engel and Wierenga, 1996).

The secondary structure elements of Hat1 are shown in Figure 2 together with the aligned sequences of Hat1 from *S. cerevisiae* and human, and HatB from maize as well as Hat1-like sequences from *Caenorhabditis elegans* and *Schizosaccharomyces pombe*. The sequences are similar over much of their length but have variable C-terminal extensions consistent with the observation that the C terminus is not required for the HAT activity of Hat1. Many of the most highly conserved residues form the hydrophobic cores of the N- or C-terminal domains or the interface between domains. We could not locate electron density for the loop between strands β13 and β14 of the C-terminal domain. This loop is also sensitive to proteolytic cleavage, indicating that it is likely to be flexible in solution. It is also the site of insertions in the sequences of the other members of the Hat1 family, which suggests that the length of the loop may vary between these proteins.

Acetyl CoA Binding and the Active Site

Hat1 binds AcCoA in a cleft toward the center of the concave surface of the protein lying approximately parallel to the six-stranded sheet of the C-terminal domain (Figures 1 and 3A). The cleft is formed by strand β14 at the edge of the sheet and the N-terminal ends of helices α8 and α9 and the C-terminal end of helix α7. Approximately 1100 Å^2 of accessible surface area is buried in the interaction. The AcCoA has a bent conformation, which allows it to wrap partially around the protein. This bend is produced mainly by a significant kink in the pantetheine group around the PC6-PC7 positions (Figure 3A) with the rest of the pantetheine group being essentially straight. This contrasts with other CoA binding proteins where bending is usually produced at the pyrophosphate group (Engel and Wierenga, 1996). Another contrast with known CoA binding proteins is that Hat1 does not seem to make intimate contact with the 3′-phosphate-adenosine (Engel and Wierenga, 1996). As mentioned earlier, we failed to detect strong density for the adenine or ribose rings although clear density corresponding to the 3′-phosphate (which is solvent exposed) could be detected. It thus seems likely that the adenosine is either flexible or exists in multiple conformations. It should be noted that the adenine ring is close to several lysine side chains of a symmetry-related molecule and may thus make a variety of transient intermolecular contacts.

About 60% of the AcCoA surface is buried, with protein–ligand contacts being made to the acetyl and pantetheine groups, and also to the pyrophosphate group that bridges the pantothenic acid and adenosine moieties. These contacts include numerous hydrophobic interactions, hydrogen bonds, and salt bridges (detailed

Table 1. Data Collection, Phasing, and Refinement Statistics

Crystal Information			
Space group	C2		
Unit cell dimensions	a = 111.3 Å, b = 47.9 Å, c = 75.7 Å, β = 90.3°		
Estimated solvent content	~45% (V_m ~2.7 Å^3/dalton)[a]		
Data Collection			
	λ_1	λ_2	λ_3 (native)
Wavelength (Å)	0.9789	0.9787	0.93
Resolution (Å)	2.3	2.3	2.3
f′ of selenium (electrons)	−9.52	−7.35	−2.19
f′′ of selenium (electrons)	3.15	5.92	3.46
I/σ (highest resolution shell)	4.3	6.6	5.29
Total reflections	172842	173843	193352
Unique reflections	18277	18252	18259
Completeness (%)	96.9	98.1	97.5
R_{sym} (total/highest resolution shell)[b]	0.035/0.145	0.04/0.127	0.034/0.139

Phasing (SOLVE)	
R_{cullis}[c]	0.56
Phasing power[d]	
centric	0.78
acentric	1.11
Figure of merit	0.58
Map correlation coefficients[e]	
SOLVE	0.5254
SOLVE + SOLOMON	0.7093

Refinement (X-plor)	
Resolution range	28.9–2.3 Å
I/σ cutoff	0.0
R[f]	0.204
R_{free}[g]	0.269
Number of nonhydrogen atoms	
Protein	2532
Acetyl CoA	51
Water molecules	113
Ca^{2+} ion	1
rms deviations from ideal geometry	
Bond lengths (Å)	0.007
Bond angles (°)	1.3

Residues within most allowed regions of Ramachandran plot (%): 99.6

[a] V_m = Matthew's coefficient (volume of asymmetric unit/molecular weight).
[b] $R_{sym} = \Sigma_h\Sigma_i| I_{ih} - <I_h> |/ \Sigma_h\Sigma_i <I_h>$, where $<I_h>$ is the mean of the observations I_{ih} of reflection h.
[c] $R_{cullis} = \Sigma|E|/\Sigma_j||F_1| - |F_{10}||$, where E is the lack of closure.
[d] Phasing power = $<|F_H(calc)|/|E|>$, where $F_H(calc)$ is the calculated anomalous difference and E is the lack of closure.
[e] Map correlation coefficient was calculated between the calculated map for the final refined model and the experimental maps before and afer solvent flattening.
[f] $R = \Sigma(||F_p(obs)| - |F_p(calc)||)/\Sigma|F_p$ (obs)|.
[g] R_{free} = R factor for a selected subset (10%) of the reflections that was not included in prior refinement calculations.

in Figure 3B). In the pantetheine region of the molecule, all but one of the potential hydrogen bonding groups of the AcCoA are involved in direct or indirect hydrogen bonds with the protein, many with the protein main chain. In general, the residues involved in AcCoA binding are clustered in three regions of the Hat1 protein: the C-terminal end of helix α7; the C-terminal end of strand β14, loop β14α8, and the N-terminal end of helix α8; and the C-terminal end of strand β15, loop β15α9, and the N-terminal half of helix α9 (Figure 2).

The acetyl group of AcCoA marks the active site of the protein. The β-methyl of the acetyl group is located in a hydrophobic pocket formed by the side chains of Ile-217, Val-254, Pro-257, Phe-261, and portions of the protein main chain from residues 217–220 and 255–256 (Figure 3C). The carbonyl oxygen of the acetyl group accepts a hydrogen bond from the main-chain amide of Phe-220 while the terminal sulphur atom of the β-mercapto-ethylamine lies within hydrogen bonding distance of the main-chain amide of Asn-258. Together these interactions help to position this end of the AcCoA molecule. Asn-258 also donates a hydrogen bond from its side-chain amide to the carbonyl oxygen PO5 at the end of the pantothenic acid group. The orientation of Asn-258 is fixed by hydrogen bonds from its side-chain amide to the main-chain amide of Glu-162 via a bridging

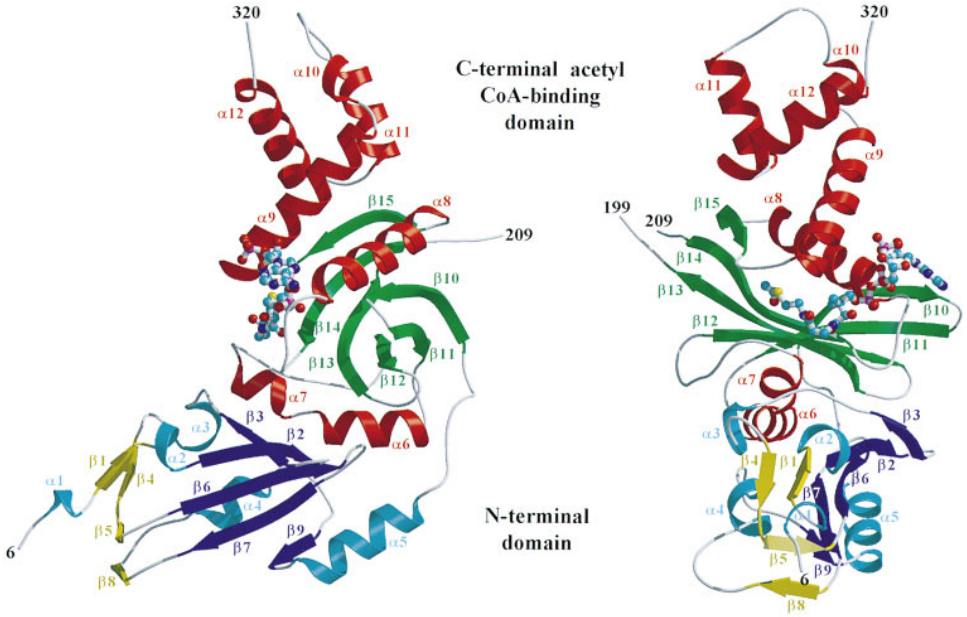

Figure 1. Overview of the Structure of the Hat1–AcCoA Complex

Schematic representation of the structure showing location of sheets and helices. The AcCoA molecule is indicated in a ball-and-stick representation. Two views of the structure are shown, related by an approximately 90° turn around the vertical axis. Figure produced using MOLSCRIPT (Kraulis, 1991) and Raster3D (Merritt and Bacon, 1997).

water molecule and a hydrogen bond from the main-chain amide of Phe-261 to its side-chain carbonyl oxygen. Together the side chains of Ile-161, Glu-162, and Asn-258 form a kind of gate that closes over the AcCoA binding cleft (Figure 3A).

The AcCoA binding site includes a βαβ structural motif whose topology resembles the Rossmann fold motif found in many nucleotide-binding proteins (Rao and Rossmann, 1973). The βαβ motif in Hat1 differs from the classical Rossmann fold in that the length of the loop prior to the helix is considerably longer and that, although the ADP portion of AcCoA is bound at the N-terminal end of the helix, it is oriented in the opposite direction. The pyrophosphate is tucked into a tight turn that precedes the N-terminal end of helix α8 (Figure 3D). This is a region of positive electrostatic surface potential arising from the side chain of Arg-267 and the N-terminal dipole of helix α8, which is also likely to contribute to AcCoA binding (Figure 3A). Many contacts are made to the phosphate oxygen atoms, mostly from main-chain amide groups of residues that are highly conserved among histone acetylases and other acetyltransferase enzymes.

It seems likely that binding of AcCoA produces a conformational change in Hat1. This conclusion is based upon our observation of a change in proteolytic sensitivity upon cofactor binding (Dutnall et al., submitted) and on our inability to grow crystals of Hat1 in the absence of AcCoA. The cleavage sites affected by AcCoA binding (around loop α10α11) lie somewhat distant from the AcCoA binding cleft, but it is plausible that a conformational change, such as closure of the protein around AcCoA, could be transmitted to this region, thereby reducing its susceptibility to cleavage.

Possible Modes of Histone Binding and Sources of Sequence Specificity

Hat1 purified from yeast extracts specifically acetylates only residue Lys-12 of histone H4 while recombinantly produced yeast Hat1 will also acetylate Lys-5 of H4 to a lesser extent and weakly acetylates histone H2A (Kleff et al., 1995; Parthun et al., 1996). Based on the activity of Hat1 on histone H4 or H2A purified from a number of species, Parthun et al. identified a common motif in the vicinity of the acetylated lysine (GxGKxG). Human Hat1 has been shown to modify Lys-5 and Lys-12 of histone H4 and, to a lesser extent, Lys-5 of H2A (assayed with recombinant *Xenopus* histones) (Verreault et al., 1998) while the HatB enzyme from maize is specific for H4 Lys-5 and Lys-12 (Eberharter et al., 1996; Kolle et al., 1998). Thus, the human and maize enzymes also conform to this recognition motif.

In order to try to gain a better understanding of the site specificity of Hat1, we attempted to model a peptide corresponding to part of the N-terminal tail of H4 into the active site (Figure 4). In the absence of any structural data for the conformation of the H4 tail around Lys-12, we constructed the peptide with an extended backbone conformation. Our primary focus in the modeling process was to bring the ε-amino group of Lys-12 into close proximity with the carbonyl group of the acetyl moiety of AcCoA as would be expected during the reaction. We next asked what constraints, if any, this placed on the orientation of the peptide and whether it revealed any clues as to the source of site specificity.

If it is assumed that no large conformational change occurs upon H4 binding, then it appears that the Lys-12 side chain can approach the carbonyl group only from one side of the gate over the AcCoA binding cleft. In an extended conformation, the lysine side chain can

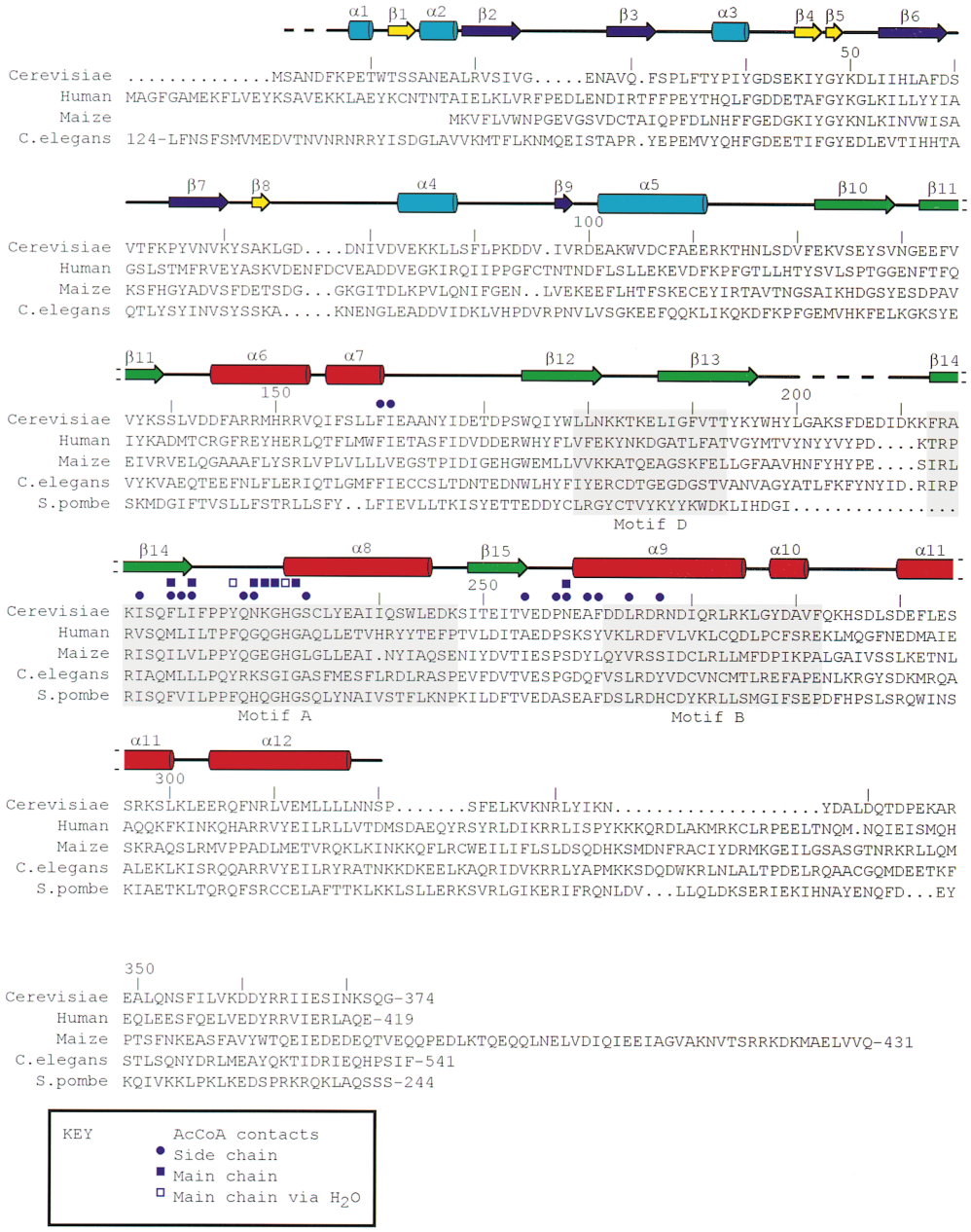

Figure 2. Secondary Structure Elements and Sequence Alignment of the Hat1 Family

The location of secondary structure elements of Hat1 is indicated above the aligned sequences of *S. cerevisiae* Hat1 (GenBank accession code U33335), human Hat1 (GenBank AF030424), maize HatB (GenBank U90274), and potential Hat1-like sequences from *C. elegans* (EMBL accession code Z49128) and *S. pombe* (EMBL Z99753). The first 124 residues of the *C. elegans* sequence are omitted for clarity. The *S. pombe* sequence is only known for a C-terminal fragment. Every tenth residue of Hat1 is indicated above the sequence. Secondary structure elements (helices indicated by cylinders, strands by arrows) are colored as in Figure 1. Dashed lines indicate regions of Hat1 for which electron density was not observed. Symbols above the sequence show the residues of Hat1 that contact AcCoA (explained in the key). Grayed boxes indicate the location of sequences conserved in the GNAT superfamily.

reach to within 1–2 Å of the carbonyl group without producing any clashes with the protein structure, particularly from the main chain either side of Lys-12. However, for a peptide with extended conformation, this can only be achieved if it traverses a cleft of varying width and depth that crosses the structure almost perpendicularly to the long axis of the protein (Figure 4).

An attractive feature of this model is that it suggests possible explanations for the length of the Hat1 recognition motif and preference for Lys-12 of histone H4. The length of the cleft is long enough to accommodate a 6–7 residue peptide in extended conformation, similar to the length of the proposed recognition motif. When the H4 peptide is orientated in the putative binding cleft as shown in Figure 4, with Lys-12 poised for modification, it brings Leu-10 adjacent to a hydrophobic pocket

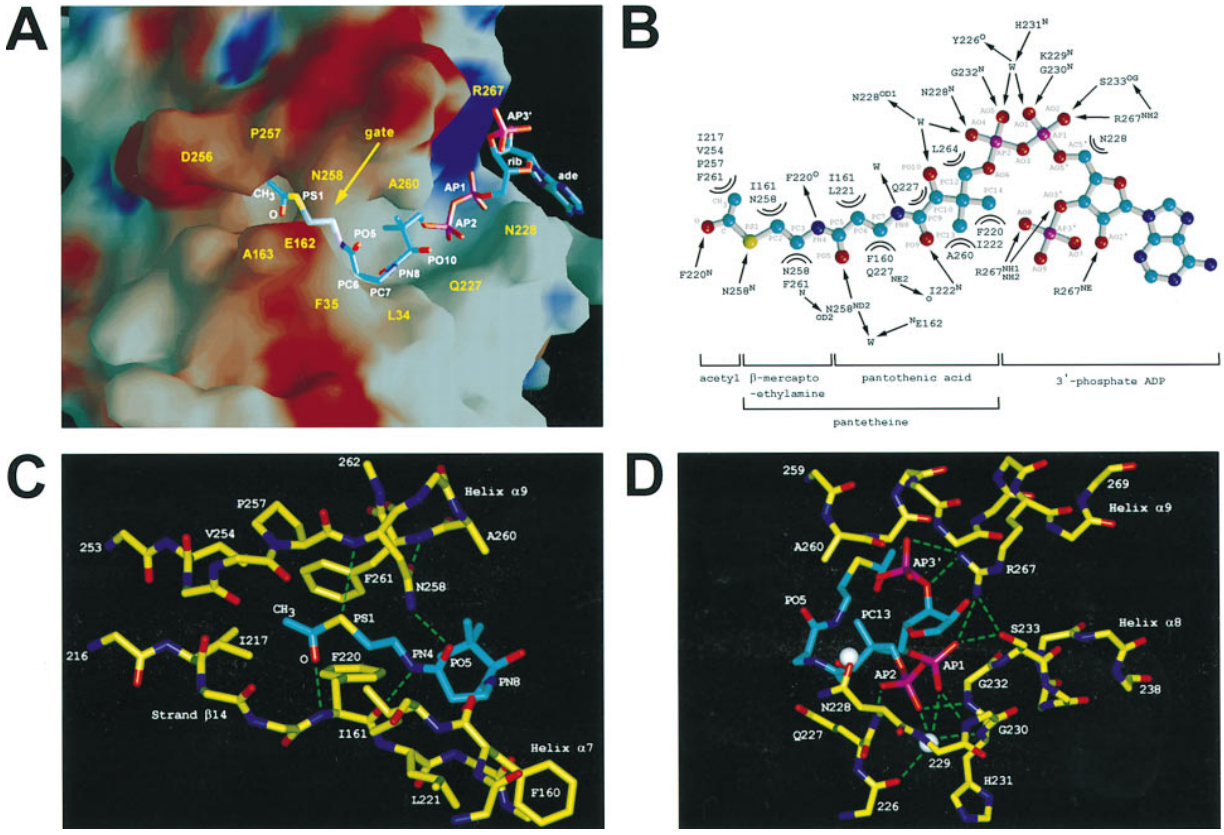

Figure 3. Hat1–Acetyl CoA Interactions

(A) Electrostatic surface potential of section of Hat1 surface around the AcCoA molecule. The potential displayed ranges from ≤ -12 to $\geq +12$ k_BT (red to blue, respectively) calculated without solvent or AcCoA molecules. The surface is partially transparent to show the AcCoA more clearly. The AcCoA is displayed in a stick representation with various functional groups labeled for reference. The approximate location of selected Hat1 residues is also indicated. Figure produced using GRASP (Nicholls et al., 1993).

(B) Schematic representation of Hat1–AcCoA contacts. The AcCoA molecule is shown stretched out for clarity with selected atoms labeled. The subcomponents of AcCoA described in the text are shown below the molecule. Hat1 residues that contact AcCoA are indicated with, in some cases, the identity of the atom taking part in the contact. Arrows indicate hydrogen bonds; concentric semicircles represent hydrophobic contacts. W, water molecule.

(C) The active site. Detailed view showing the location of the acetyl group in a hydrophobic pocket and contacts to the proximal end of the pantetheine arm. Selected side chains and portions of the protein main chain of Hat1 along with regions of the AcCoA molecule are shown in stick representation. The start and end of main-chain segments are indicated along with the position of elements of secondary structure. Hydrogen bonds are indicated by green dashed lines. Water molecules are shown as white spheres.

(D) Pyrophosphate contacts from the conserved glycine residues at the start of helix α9.

that forms the deepest part of the cleft. Positioning Leu-10 of H4 in this pocket may contribute to selectivity for Lys-12. It also places Gly-13 and Gly-14 in the shallowest and narrowest part of the cleft (Figure 4), which may explain the preference for glycine residues at these positions of the recognition motif. One last additional source of preference for Lys-12 of histone H4 may arise from interactions with the nonmodified lysine residues on either side of this site (Lys-8 and Lys-16). In the current model, these side chains are adjacent to acidic patches on the surface of the protein, which could add binding energy through electrostatic interactions.

Our model also provides possible explanations for the lower activity of Hat1 on histone H4 Lys-5 and H2A Lys-5. If H4 Lys-5 is positioned in the active site, it places an arginine side chain (Arg-3) in the hydrophobic pocket. This would presumably be a less favorable interaction but may be accommodated partly by flexibility in the peptide main chain provided by glycines on either side of this residue. When H2A Lys-5 is poised for modification, it not only places an arginine in the hydrophobic pocket, but also places a glutamine side chain in the narrowest part of the cleft, which may explain the further relative reduction in the ability of Hat1 to modify this site when compared with H4 Lys-12 or Lys-5. This type of poor structural complementarity may also explain the inability of Hat1 to modify either H4 Lys-8 or Lys-16. Placing these side chains in the active site causes Leu-10 or His-18, respectively, to clash with the shallow part of the cleft and, in addition, does not place a suitable side chain for interaction in the hydrophobic pocket.

In general, our model proposes that at least part of the substrate specificity of Hat1 may arise from a complementary fit of the recognition motif around the lysine to be modified with features of the surface of Hat1. Additional specificity may come from the interaction of

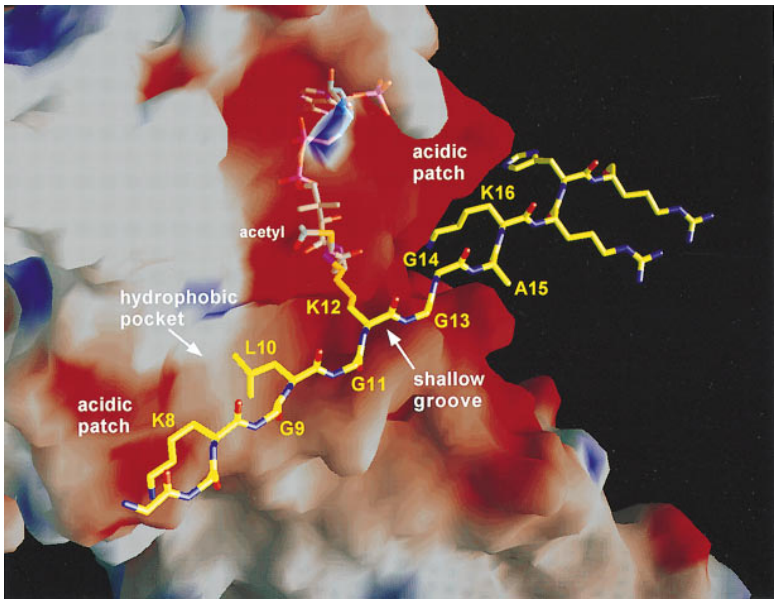

Figure 4. Model of Histone H4 Tail Binding Suggests How a Complementary Fit May Explain Substrate Recognition by Hat1

An electrostatic surface potential of the Hat1–AcCoA complex is shown along with a stick representation of the AcCoA and H4 peptide (residues 6–19). The surface is partially transparent to show the location of the acetyl group and the side chain of Lys-12 positioned for modification. The surface features of Hat1 that may play a role in substrate recognition are indicated.

Hat1 with its accessory protein Hat2 (Parthun et al., 1996). It also raises the possibility that modifications of residues within the recognition site (for example, acetylation of H4 Lys-8 or Lys-16) could modulate the ability of Hat1 to modify H4 Lys-12 and in general suggests that the activities of various histone acetylase and deacetylase enzymes may be coupled in some way via their overlapping recognition sites.

Possible Modes of Catalysis

AcCoA carries the acetyl group in an activated state, attached via a high-energy thioester bond whose hydrolysis is thermodynamically more favorable than that of an oxygen ester. AcCoA thus has a high acetyl group transfer potential (Stryer, 1995). One possible reaction mechanism involves a two-step process whereby the acetyl group is first transferred to a group on the enzyme and then subsequently transferred to the histone substrate producing an acetylated enzyme intermediate (Wong and Wong, 1983). Hat1 contains two cysteine residues, which would be the most obvious sites to accept an acetyl group, but both are too far away from the AcCoA. Furthermore, we have been unable to detect any evidence of such an intermediate (S. T. T and R. S., unpublished data).

In the Hat1 structure, the closest residue whose side chain could possibly play a catalytic role is Asn-258, but this is not conserved with other Hat1 family members, and its location does not immediately suggest how it could be involved in catalysis. Instead, it is possible that a lone pair on the ϵ-amino group of the lysine to be modified makes a direct nucleophilic attack on the carbonyl carbon of the acetyl group to initiate an acyl transfer reaction. This mechanism would form a tetravalent intermediate, and some support for this type of reaction comes from the inhibitory effects of the multisubstrate analog N-[2-(S-Coenzyme A)acetyl] spermidine amide on HAT activities from calf thymus and rat liver (Cullis et al., 1982; Erwin et al., 1984). This mechanism would also require the lysine to be uncharged. While lysines at physiological pH are normally charged, it is possible that the environment of the catalytic site stabilizes an uncharged state or that a proton from the lysine is donated to some group on the protein during substrate binding. Hat1 could facilitate transfer by ordering the substrates for reaction. The Hat1–AcCoA complex shows that the enzyme makes several important contacts that locate the acetyl group in the active site. From the model of the peptide bound to Hat1 described above, it is also possible to see how the enzyme could orient the ϵ-amino group of the lysine. If the ϵ-amino group is brought to within 2 Å of the acetyl group, it is close enough to make hydrogen bonds with several main-chain carbonyl groups. The entropic cost of ordering the reactants would then be balanced in part by the binding energy.

The structure and limited proteolysis of Hat1 suggest that AcCoA binding produces a conformational change in the enzyme. This suggests that AcCoA binds first and that the subsequent conformational change in Hat1 sets up the histone binding site. Based on the peptide binding model described in the previous section, it is difficult to imagine how AcCoA could bind after histone. We have also observed that incubation of an H4 peptide with Hat1 produces no significant change in the proteolysis pattern of Hat1 (R. N. D. and V. R., unpublished data).

A Structural Paradigm for an Acetyltransferase Superfamily

The structure of Hat1 sheds light on its relationship to other histone acetyltransferases and improves the basis of comparison to those proteins that have only a low degree of sequence similarity. As shown below, this leads to a modification of the sequence alignments proposed earlier. Most of the known HAT enzymes share conserved sequence motifs with each other and with a more extended superfamily, called the GCN5-related N-acetyltransferase (GNAT) superfamily, which includes protein N-acetyltransferases (NATs), metabolic enzymes, detoxification and drug resistance enzymes, and other

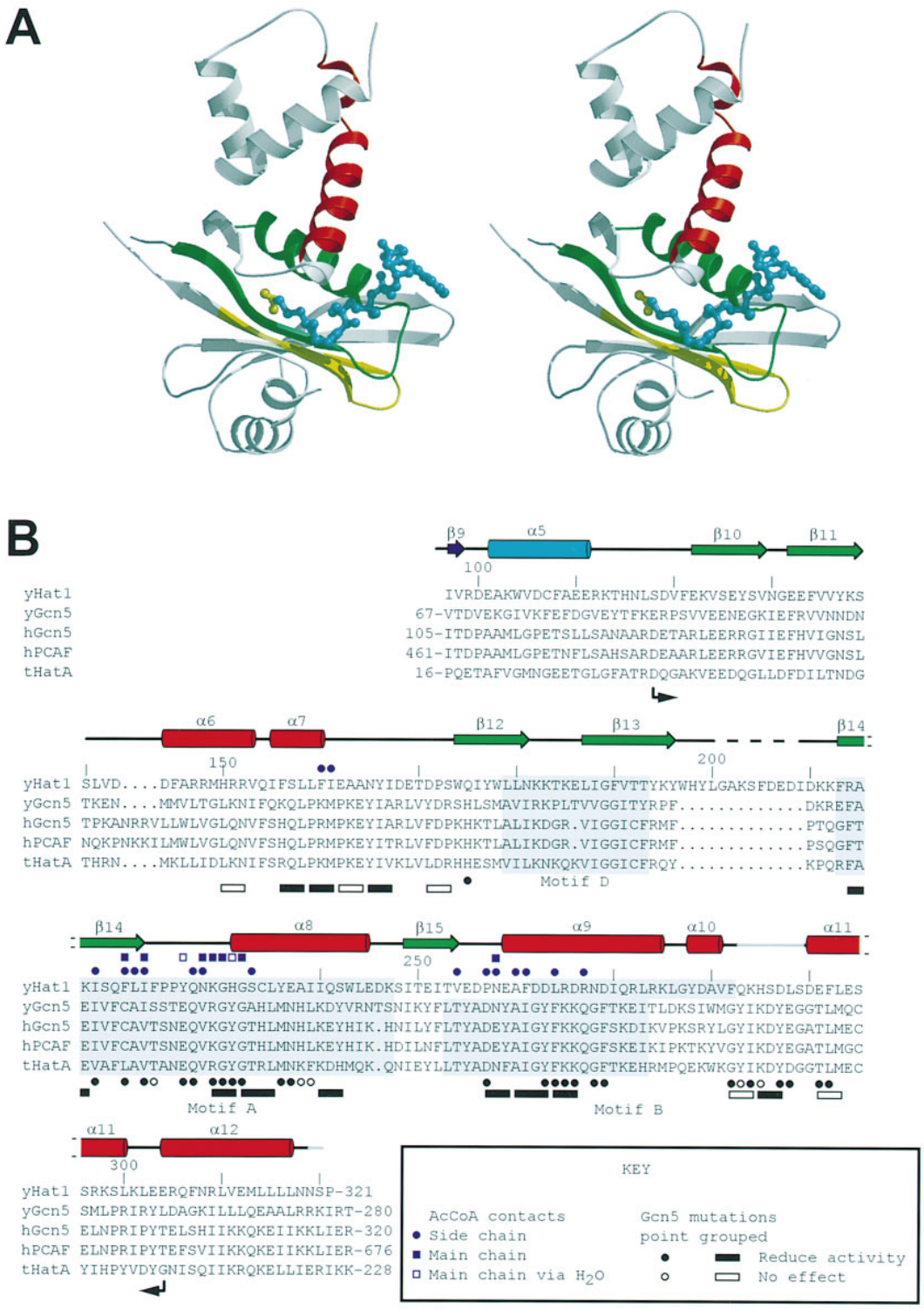

Figure 5. Relationship of the Hat1 Structure to the GNAT Superfamily

(A) Stereo view of the C-terminal domain of Hat1 with the location of the GNAT conserved sequence motifs highlighted. Green, motif A; red, motif B; yellow, motif D. AcCoA is shown as a ball-and-stick representation with CoA colored cyan and the acetyl group colored yellow. The orientation is similar to that shown in the right panel of Figure 1.

(B) Alignment of C-terminal domain of Hat1 with the HAT domain of the Gcn5 family. Sections of the sequences of yeast and human Gcn5, human P/CAF (hPCAF), and *Tetrahymena* HatA are shown. The borders of the HAT domain of yGcn5 are indicated by arrows below the alignment. Other symbols are explained in the key.

proteins whose function is unknown (Tercero et al., 1992; Reifsnyder et al., 1996; Neuwald and Landsman, 1997). Among the HAT enzymes included in this superfamily are Hat1 and its homologs, the Gcn5 family of proteins (which includes P/CAF and *T. thermophila* Hat-A [Brownell et al., 1996; Yang et al., 1996] and the Esa1 family (which includes Sas2, Sas3, MOF, MOZ, and Tip60 [Reifsnyder et al., 1996; Smith et al., 1998]). Neuwald and Landsman (1997) have described four conserved sequence motifs (A–D) to characterize the GNAT superfamily. Of these, motif A is the longest and most highly conserved. According to this scheme, the HAT families lack motif C, and the Esa1 family appears to contain motifs A and B in reverse order (see Kuo et al., 1998). The location of these motifs in the Hat1 structure is shown in Figure 5A (see also Figure 2). It was previously suggested that these conserved motifs are involved in AcCoA binding (Neuwald and Landsman, 1997). The structure of Hat1 shows that, indeed, these structural motifs make up a large part of the AcCoA binding region.

Within the conserved sequence motifs are several highly conserved residues, several of which have been shown to be important for function by mutagenesis of the NAT enzymes Mak3 from yeast and the human spermine/spermidine NAT (SSAT), and the HAT enzymes Gcn5 and Esa1. Of particular interest is the motif Q/RxxGxG (where x is any amino acid) within motif A. Point mutations of any of these conserved residues lead to a greater than 95% reduction in the activity of SSAT (Coleman et al., 1996; Lu et al., 1996) while for Gcn5, mutations anywhere in this motif reduce the activity of the enzyme by greater than 90% (Kuo et al., 1998). Mutation of the central glycine residue of this motif abolishes the function of the *MAK3* gene (Tercero et al., 1992), virtually abolishes in vitro HAT activity of Esa1 (Smith et al., 1998), and causes a mutant phenotype of the *Drosophila MOF* gene (Hilfiker et al., 1997). The Hat1 structure shows that the Q/RxxGxG motif makes up an important part of the pyrophosphate-binding loop (Figure 3D). The strong conservation of the two glycine residues implies that replacement with large side chains disrupts the structure of this loop, thereby severely reducing AcCoA binding affinity as has been observed for SSAT (Lu et al., 1996).

Mutation of Mak3 residues Phe-94 or Val-96 also abolishes the function of this protein (Tercero et al., 1992). These two residues, which correspond to Hat1 residues Phe-220 and Ile-222, are highly conserved in the GNAT superfamily (occupied by hydrophobic residues). In Hat1, Phe-220 and Ile-222 make important contributions to binding of AcCoA. In particular, Phe-220 makes two hydrogen bonds via its main chain to the amide nitrogen PN4 and the carbonyl oxygen of the acetyl group (Figure 3C). Mutation of Phe-220 could disrupt the formation of these hydrogen bonds, which may be critical for positioning of the acetyl group in the active site.

What is the relevance of the Hat1 structure for other histone acetyltransferases such as Gcn5? In Figure 5B, we show an alignment of the HAT domain of Hat1 with corresponding parts of the Gcn5 family using the Hat1 structure as a guide along with the GNAT conserved motifs D and A. The alignment places a large insertion in Hat1 between motifs D and A (corresponding to Hat1 loop $\beta13\beta14$), which seems reasonable, as it appears that the length of this loop is variable in the Hat1 family. We also note that yeast and human Gcn5 and P/CAF have a proline residue within this loop, which would be ideal for constructing a tighter turn between strands $\beta13$ and $\beta14$.

We did not align Hat1 and the Gcn5 family according to motif B of Neuwald and Landsman (1997) for the following reason. In their alignment, the distance between motifs A and B in Hat1 is 14 residues, while for the Gcn5 family this distance is only 4 or 5 residues. If this region is conserved because it forms an important structural motif (helix $\alpha9$), and this motif has a similar orientation in Hat1 and Gcn5, then the shorter distance between motifs A and B in Gcn5, as defined, would place severe strain on the structure. We therefore simply aligned the Hat1 and Gcn5 sequences with no insertions in Hat1 from the end of motif A onward. It should be noted that our alignment of Hat1 and Gcn5 results in a similar level of sequence similarity in the region of the previously defined motif B of Hat1 or Gcn5 (see Figure 5B).

Our alignment results in a striking outcome when the data from two recent alanine scanning mutagenesis studies on yeast Gcn5 (yGcn5) are considered (Kuo et al., 1998; Wang et al., 1998). Many of the mutations that affect yGcn5 activity map to residues of Hat1 that are involved in AcCoA binding (Figures 5B and 6) while others can be explained by their probable effects on the stability of the structure. The correspondence within motif A is to be expected given the degree of similarity within the GNAT family in this region. As described earlier, the Q/RxxGxG motif is critical for function as are the positions corresponding to Hat1 residues Phe-220 and Ile-222 (see Figure 5B). Mutations of the residue corresponding to Hat1 Ile-217 also reduce yGcn5 HAT activity. Ile-217 forms part of the hydrophobic pocket that surrounds the methyl group of the acetyl moiety in AcCoA. Mutating this residue to alanine would increase the size of this pocket and perhaps place less constraint on the orientation of the acetyl group, which in turn may affect catalysis.

A second cluster of Gcn5 mutations that affect activity maps to the region around the N-terminal end of helix $\alpha9$ (Figure 5B), which also contains Hat1 AcCoA binding residues. Many of these AcCoA binding residues are conserved in Gcn5, and thus, reduction of Gcn5 activity is likely to be a consequence of reducing AcCoA binding affinity. Other residues in this region of yGcn5 that affect activity when mutated correspond to residues that would be expected to contribute to the stability of the structure.

Another cluster of residues important for yGcn5 activity lies in the region N-terminal to motif D, and the correspondence of this region with a region of Hat1 involved in AcCoA binding (C terminus of helix $\alpha7$) is striking. It should be noted that this region contains residues that are highly conserved within either the Hat1 family or the Gcn5 family but not between these families (Figures 2 and 5B). This region may also contain residues of Hat1 involved in histone binding, and the reason for conservation within but not between families may thus be related to the different substrate specificity of these two families of HAT enzymes (Kuo et al., 1996).

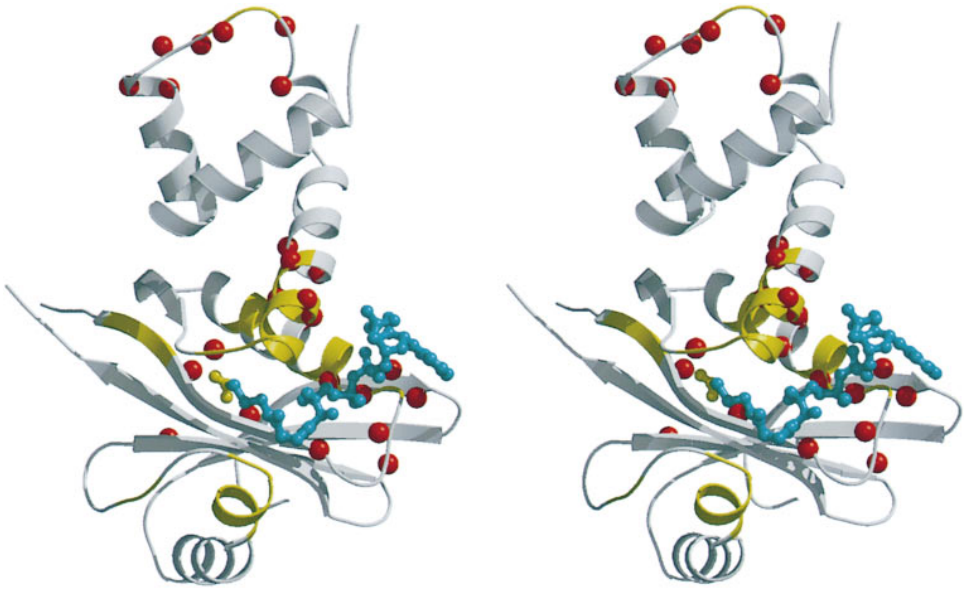

Figure 6. Structural Location of Gcn5 Mutations that Reduce HAT Activity

Stereo view of the C-terminal domain of Hat1 with the AcCoA colored as in Figure 5A. Using the alignment in Figure 5B, the C_α atoms of residues of Hat1 that correspond to residues that reduce Gcn5 activity when changed to alanine as point mutations are shown as red spheres. Likewise, the backbone of segments of residues that reduce Gcn5 activity when changed to alanine as grouped mutations are shown in yellow.

Since the regions of Hat1 involved in AcCoA binding correspond well with mutations that affect yGcn5 activity, we propose that the structure of that HAT domain of the Gcn5 family closely resembles the C-terminal domain of Hat1. Further evidence in support of such a hypothesis is provided by a study that identified residues between 95 and 261 of yGcn5 to be required for full HAT activity in vitro (Candau et al., 1997). Based on the alignment in Figure 5B, the borders of the yGcn5 HAT domain would include nearly all of the C-terminal domain of Hat1 (from strand β10 up to, and including, helix α11).

It has recently been noted that the HAT domains of P/CAF and CBP share sequence similarity (Martinez-Balbas et al., 1998). CBP was not initially identified as a member of the GNAT family presumably because the degree of sequence similarity falls below the detection level employed in previous searches. In addition, Martinez-Balbas et al. (1998) identify several residues that reduce the HAT activity of CBP when mutated, most of which have a rational basis in terms of the Hat1 structure. Significantly, as for yGcn5, some of these mutations lie N-terminal to motif D. Thus, the HAT domain of CBP may also resemble the C-terminal domain of Hat1. Future structural studies of other less well-related HAT enzymes and other members of the GNAT superfamily will be needed to examine the relationship between their structures and to correlate this with their diverse substrate specificities and biological functions.

Conclusions

The structure of Hat1 shows how the enzyme binds AcCoA, and it suggests possible modes of histone substrate recognition and catalysis. Importantly, the structure provides a framework for understanding functional analysis of the catalytic domains of a superfamily of acetyltransferases and suggests an explanation for the mutagenesis data on other HAT enzymes, such as Gcn5 and CBP, whose catalytic domains are likely to be structurally related to that of Hat1.

In addition, the structure of Hat1 described here provides several directions for future studies on its function. The model proposed for substrate recognition and catalysis can be tested by studies on the complex of Hat1 with a substrate peptide, with substrate analogs, and by site-directed mutagenesis. It should be remembered that in vivo, Hat1, like many other histone acetyltransferases, has at least one partner, Hat2, that stimulates HAT activity. Structural and biochemical studies on the complex of Hat1 with Hat2 are needed to understand the role of Hat2 in the biology of histone acetylation by Hat1.

Experimental Procedures

Expression and Purification of Hat1 Protein

Full-length and C-terminal deletion constructs of Hat1 were expressed in *Escherichia coli* using the T7 polymerase expression system (Studier et al., 1990) in the *E. coli* strain BL21 (DE3), using the expression vector pET13a (Gerchman et al., 1994). In order to produce selenomethionine-substituted protein, the *E. coli* strain B834(DE3), a methionine auxotroph, was used, and the cells were grown in minimal medium supplemented with amino acids, vitamins, and seleno-L-methionine as described previously (Ramakrishnan et al., 1993).

Each Hat1 construct was purified from soluble cell extracts by a combination of anion exchange, hydroxyapatite, and gel filtration chromatography and checked by N-terminal sequencing and mass spectrometry. The histone acetylase activity of the truncated proteins was compared with full-length recombinant Hat1 by liquid assays with histone H4 (1–28) peptide monitored by scintillation counting and with a mixture of chicken erythrocyte histones monitored by SDS-PAGE and fluorography as previously described (Kleff et al., 1995; Parthun et al., 1996).

Crystal Growth and Data Collection

Hat1 protein was dialyzed into 5 mM HEPES (pH 7.6), 1 mM DTT before concentrating to 10–20 mg/ml. Crystals were grown by the hanging drop vapor diffusion method. Diffraction quality crystals were prepared by preincubating the protein at 10 mg/ml with a 2-fold molar excess of AcCoA in 2.5 mM HEPES (pH 7.6), 0.5 mM DTT, 0.1 M $CaCl_2$ for 1 hr at room temperature. The reservoir solution contained 12% (w/v) PEG400, 0.1 M Tris·Cl (pH 8.0 or 8.5), and drops were set up with 2 μl protein solution plus 2 μl reservoir solution at 4°C. Crystals appeared within 24 hr and grew to their final size (up to 1 mm × 0.4 mm × 0.4 mm) in 3–4 days. For X-ray diffraction analysis, crystals were slowly transferred in a stepwise fashion into a cryoprotectant solution containing 30% (w/v) PEG400, 0.1 M Tris·Cl (pH 8.0 or 8.5), 0.27 mM AcCoA before flash freezing in liquid nitrogen.

A 3-wavelength MAD data set was collected on a single crystal of selenomethionine-substituted Hat1(1–320) on beamline X12-C at the National Synchrotron Light Source at Brookhaven National Laboratory. The crystal was maintained at 100 K using an Oxford Cryostream, and data were collected in 1° oscillations using a 20 × 20 cm CCD detector (Stanton et al., 1994). The first and second wavelengths, λ1 and λ2, were at the inflection point and peak of the K-edge of selenium at 0.9789 Å and 0.9787 Å, respectively, while the third, λ3, was a remote wavelength at 0.93 Å (each wavelength was collected in a single sweep). Data were integrated and scaled using the programs Denzo and Scalepack (Otwinowski and Minor, 1997).

Phasing and Refinement

The MAD data were phased by treating one of the wavelengths (λ3) as "native" or reference wavelength and the other wavelengths as "derivative" (Ramakrishnan and Biou, 1997) using a Bayesian approach in which the three wavelengths were reduced to single isomorphous and anomalous scattering contributions (Terwilliger, 1997). Inspection of an anomalous Patterson map calculated using the λ2 data clearly indicated the presence of two selenium peaks per asymmetric unit. The program SOLVE (see http://www.solve.lanl.gov/) was used to reduce automatically the integrated, scaled intensities to structure factors, perform local scaling with respect to the reference wavelength, solve for the heavy atom positions, and refine heavy atom phases. The phases produced by SOLVE were used to calculate an electron density map using the CCP4 package and solvent flattened using the program SOLOMON assuming a solvent content of 45% (Abrahams and Leslie, 1996; Collaborative Computational Project Number 4, 1994). The final solvent-flattened map was of excellent quality, with a correlation coefficient of 0.71 relative to the final refined model.

An initial model for 295 of the 319 protein residues could be built into the solvent-flattened map using the program O (Jones et al., 1991). Refinement was carried out using the λ3 data from 6.0–2.3 Å in the program X-plor (Brünger, 1996). In all calculations, Bijvoet pairs were kept separate, and the anomalous scattering terms of selenium were included in the calculation of structure factors. After an initial round of positional, grouped B factor and torsion angle refinement, AcCoA was added to the model. Refinement proceeded by rounds of positional, grouped B factor and simulated annealing interspersed with inspection and adjustment of the model with reference to $2f_o - f_c$ and $f_o - f_c$ maps. In the final stages of refinement, a bulk solvent correction was applied, and the structure refined against all the data (28.9–2.3 Å). Finally, solvent molecules were added and only retained if density could be observed for them, if possible H-bond partners could be located within a reasonable distance, and if they refined to a B factor lower than 70 $Å^2$.

Acknowledgments

We thank Robert M. Sweet for help and advice with data collection, Sue-Ellen Gerchman for constructing the expression clone for full-length Hat1, and Robert Schackmann for help with N-terminal sequencing. We would also like to thank Brian Wimberly and Jacqui Wittmeyer for critical comments on the manuscript. This work was supported by NIH grants GM 42796 (to V. R.), and GM28220 and GM55641 (to R. S.), and a Funding Incentive Seed Grant from the University of Utah (to V. R.). Beamline X12C at the NSLS at Brookhaven is supported by the United States Department of Energy Offices of Health and Environmental Research and of Basic Energy Sciences, and by the National Science Foundation.

Received May 29, 1998; revised July 8, 1998.

References

Abrahams, J.P., and Leslie, A.G.W. (1996). Methods used in the structure determination of bovine mitochondrial F_1ATPase. Acta Crystallogr. D *52*, 30–42.

Brownell, J.E., and Allis, C.D. (1996). Special HATs for special occasions: linking histone acetylation to chromatin assembly and gene activation. Curr. Opin. Genet. Dev. *6*, 176–184.

Brownell, J.E., Zhou, J., Ranalli, T., Kobayashi, R., Edmondson, D.G., Roth, S.Y., and Allis, C.D. (1996). *Tetrahymena* histone acetyltransferase A: a homolog to yeast Gcn5p linking histone acetylation to gene activation. Cell *84*, 843–851.

Brünger, A.T. (1996). X-PLOR Version 3.843: A system for X-Ray Crystallography and NMR (New Haven, CT: Yale University Press).

Candau, R., Zhou, J.X., Allis, C.D., and Berger, S.L. (1997). Histone acetyltransferase activity and interaction with ADA2 are critical for GCN5 function in vivo. EMBO J. *16*, 555–565.

Coleman, C.S., Huang, H., and Pegg, A.E. (1996). Structure and critical residues at the active site of spermidine/spermine-N1-acetyltransferase. Biochem. J. *316*, 697–701.

Collaborative Computational Project Number 4 (1994). The CCP4 suite: programs for protein crystallography. Acta Crystallogr. D *50*, 760–763.

Cullis, P.M., Wolfenden, R., Cousens, L.S., and Alberts, B.M. (1982). Inhibition of histone acetylation by N-[2-(S-coenzyme A)acetyl] spermidine amide, a multisubstrate analog. J. Biol. Chem. *257*, 12165–12169.

Eberharter, A., Lechner, T., Goralik-Schramel, M., and Loidl, P. (1996). Purification and characterization of the cytoplasmic histone acetyltransferase B of maize embryos. FEBS Lett. *386*, 75–81.

Engel, C., and Wierenga, R. (1996). The diverse world of coenzyme A binding proteins. Curr. Opin. Struct. Biol. *6*, 790–797.

Erwin, B.G., Persson, L., and Pegg, A.E. (1984). Differential inhibition of histone and polyamine acetylases by multisubstrate analogues. Biochemistry *23*, 4250–4255.

Gerchman, S.E., Graziano, V., and Ramakrishnan, V. (1994). Expression of chicken linker histones in *E. coli*: sources of problems and methods for overcoming some of the difficulties. Protein Expr. Purif. *5*, 242–251.

Grunstein, M. (1997). Histone acetylation in chromatin structure and transcription. Nature *389*, 349–352.

Hilfiker, A., Hilfiker-Kleiner, D., Pannuti, A., and Lucchesi, J.C. (1997). mof, a putative acetyl transferase gene related to the *Tip60* and *MOZ* human genes and to the *SAS* genes of yeast, is required for dosage compensation in *Drosophila*. EMBO J. *16*, 2054–2060.

Jones, T.A., Zou, J.Y., Cowan, S.W., and Kjeldgaard (1991). Improved methods for building protein models in electron density maps and the location of errors in these models. Acta Crystallogr. A *47*, 110–119.

Kadonaga, J.T. (1998). Eukaryotic transcription: an interlaced network of transcription factors and chromatin-modifying machines. Cell *92*, 307–313.

Kaufman, P.D. (1996). Nucleosome assembly: the CAF and the HAT. Curr. Opin. Cell Biol. *8*, 369–373.

Kaufman, P.D., Kobayashi, R., and Stillman, B. (1997). Ultraviolet radiation sensitivity and reduction of telomeric silencing in *Saccharomyces cerevisiae* cells lacking chromatin assembly factor-I. Genes Dev. *11*, 345–357.

Kleff, S., Andrulis, E.D., Anderson, C.W., and Sternglanz, R. (1995). Identification of a gene encoding a yeast histone H4 acetyltransferase. J. Biol. Chem. *270*, 24674–24677.

Kolle, D., Sarg, B., Lindner, H., and Loidl, P. (1998). Substrate and

sequential site specificity of cytoplasmic histone acetyltransferases of maize and rat liver. FEBS Lett. *421*, 109–114.

Kraulis, P.J. (1991). MOLSCRIPT—a program to produce both detailed and schematic plots of protein structures. J. Appl. Crystallogr. *24*, 946–950.

Kuo, M.H., Brownell, J.E., Sobel, R.E., Ranalli, T.A., Cook, R.G., Edmondson, D.G., Roth, S.Y., and Allis, C.D. (1996). Transcription-linked acetylation by Gcn5p of histones H3 and H4 at specific lysines. Nature *383*, 269–272.

Kuo, M.H., Zhou, J., Jambeck, P., Churchill, M.E., and Allis, C.D. (1998). Histone acetyltransferase activity of yeast Gcn5p is required for the activation of target genes in vivo. Genes Dev. *12*, 627–639.

Lu, L., Berkey, K.A., and Casero, R.A., Jr. (1996). RGFGIGS is an amino acid sequence required for acetyl coenzyme A binding and activity of human spermidine/spermine N1 acetyltransferase. J. Biol. Chem. *271*, 18920–18924.

Martinez-Balbas, M.A., Bannister, A.J., Martin, K., Haus-Seuffert, P., Meisterernst, M., and Kouzarides, T. (1998). The acetyltransferase activity of CBP stimulates transcription. EMBO J. *17*, 2886–2893.

Merritt, E.A., and Bacon, D.J. (1997). Raster3D: photorealistic molecular graphics. Methods Enzymol. *277*, 505–524.

Neer, E.J., Schmidt, C.J., Nambudripad, R., and Smith, T.F. (1994). The ancient regulatory-protein family of WD-repeat proteins. Nature *371*, 297–300.

Neuwald, A.F., and Landsman, D. (1997). GCN5-related histone N-acetyltransferases belong to a diverse superfamily that includes the yeast SPT10 protein. Trends Biochem. Sci. *22*, 154–155.

Nicholls, A., Bharadwaj, R., and Honig, B. (1993). GRASP: graphical representation and analysis of surface properties. Biophys. J. *64*, 166–170.

Otwinowski, Z., and Minor, W. (1997). Processing of X-ray diffraction data collected in oscillation mode. In Methods in Enzymology, C.W. Carter, Jr., and R.M. Sweet, eds. (New York: Academic Press), pp. 307–325.

Parthun, M.R., Widom, J., and Gottschling, D.E. (1996). The major cytoplasmic histone acetyltransferase in yeast: links to chromatin replication and histone metabolism. Cell *87*, 85–94.

Ramakrishnan, V., and Biou, V. (1997). Treatment of multiwavelength anomalous diffraction data as a special case of multiple isomorphous replacement. In Methods in Enzymology, C.W. Carter, Jr., and R.M. Sweet, eds. (New York: Academic Press), pp. 538–557.

Ramakrishnan, V., Finch, J.T., Graziano, V., Lee, P.L., and Sweet, R.M. (1993). Crystal structure of globular domain of histone H5 and its implications for nucleosome binding. Nature *362*, 219–223.

Rao, S.T., and Rossmann, M.G. (1973). Comparison of super-secondary structures in proteins. J. Mol. Biol. *76*, 241–256.

Reifsnyder, C., Lowell, J., Clarke, A., and Pillus, L. (1996). Yeast *SAS* silencing genes and human genes associated with AML and HIV-1 Tat interactions are homologous with acetyltransferases. Nat. Genet. *14*, 42–49.

Richman, R., Chicoine, L.G., Collini, M.P., Cook, R.G., and Allis, C.D. (1988). Micronuclei and the cytoplasm of growing *Tetrahymena* contain a histone acetylase activity which is highly specific for free histone H4. J. Cell Biol. *106*, 1017–1026.

Roth, S.Y., and Allis, C.D. (1996). Histone acetylation and chromatin assembly: a single escort, multiple dances? Cell *87*, 5–8.

Ruiz-García, A.B., Sendra, R., Galiana, M., Pamblanco, M., Perez-Ortín, J.E., and Tordera, V. (1998). HAT1 and HAT2 proteins are components of a yeast nuclear histone acetyltransferase enzyme specific for free histone H4. J. Biol. Chem. *273*, 12599–12605.

Smith, E.R., Eisen, A., Gu, W., Sattah, M., Pannuti, A., Zhou, J., Cook, R.G., Lucchesi, J.C., and Allis, C.D. (1998). ESA1 is a histone acetyltransferase that is essential for growth in yeast. Proc. Natl. Acad. Sci. USA *95*, 3561–3565.

Sobel, R.E., Cook, R.G., Perry, C.A., Annunziato, A.T., and Allis, C.D. (1995). Conservation of deposition-related acetylation sites in newly synthesized histones H3 and H4. Proc. Natl. Acad. Sci. USA *92*, 1237–1241.

Stanton, M., Phillips, W.C., and O'Mara, D. (1994). CCD-based detector for X-ray crystallography. Proc. Soc. Photo-Opt. Instr. Eng. *2278*, 16–20.

Struhl, K. (1998). Histone acetylation and transcriptional regulatory mechanisms. Genes Dev. *12*, 599–606.

Stryer, L. (1995). Biochemistry, 4th edition (New York: W.H. Freeman).

Studier, F.W., Rosenberg, A.H., Dunn, J.J., and Dubendorff, J.W. (1990). Use of T7 RNA polymerase to direct expression of cloned genes. Methods Enzymol. *185*, 61–89.

Tercero, J.C., Riles, L.E., and Wickner, R.B. (1992). Localized mutagenesis and evidence for post-transcriptional regulation of MAK3. A putative N-acetyltransferase required for double-stranded RNA virus propagation in *Saccharomyces cerevisiae*. J. Biol. Chem. *267*, 20270–20276.

Terwilliger, T.C. (1997). Multiwavelength anomalous diffraction phasing of macromolecular structures: analysis of MAD data as single isomorphous replacement with anomalous scattering data using the MADMRG Program. Methods Enzymol. *276*, 530–537.

Turner, B.M. (1998). Histone acetylation as an epigenetic determinant of long-term transcriptional competence. Cell Mol. Life Sci. *54*, 21–31.

Verreault, A., Kaufman, P.D., Kobayashi, R., and Stillman, B. (1996). Nucleosome assembly by a complex of CAF-1 and acetylated histones H3/H4. Cell *87*, 95–104.

Verreault, A., Kaufman, P.D., Kobayashi, R., and Stillman, B. (1998). Nucleosomal DNA regulates the core-histone-binding subunit of the human Hat1 acetyltransferase. Curr. Biol. *8*, 96–108.

Wang, L., Liu, L., and Berger, S.L. (1998). Critical residues for histone acetylation by Gcn5, functioning in Ada and SAGA complexes, are also required for transcriptional function in vivo. Genes Dev. *12*, 640–653.

Wong, L.J., and Wong, S.S. (1983). Kinetic mechanism of the reaction catalyzed by nuclear histone acetyltransferase from calf thymus. Biochemistry *22*, 4637–4641.

Yang, X.J., Ogryzko, V.V., Nishikawa, J., Howard, B.H., and Nakatani, Y. (1996). A p300/CBP-associated factor that competes with the adenoviral oncoprotein E1A. Nature *382*, 319–324.

Brookhaven Protein Database Accession Number

The accession number for the coordinates of the structure reported in this paper is 1BOB. Until their release, requests for coordinates may be addressed to the authors (e-mail to rnd@snowbird.med.utah.edu).